

Electronic Supplementary Information

Easy patterning of silver nanoparticle superstructures on silicon surfaces

Chao Li, Zhiyong Tang* and Lei Jiang

Experimental Methods

Silicon-supported Ag SSs: P <100> silicon wafers were cut into 0.5 cm × 0.5 cm small pieces, then cleaned by ultrasound in acetone, ethanol, and deionized water in turn and dried by N₂ flow. One group of cleaned silicon wafers were directly dipped into 150 mL Ag⁺/Cys coordination aqueous solution with the concentration of 0.15 mM Ag⁺ and 0.25 mM Cys and the pH value of about 10.40-10.50 adjusted by 2 M NaOH aqueous solution. Another group of cleaned silicon wafers were pretreated in HF acid (40%, 30 min) and then put into the Ag⁺/Cys coordination solution under the same conditions. Then, the solutions were kept at 37 °C for 2 days. After reaction, the wafers were rinsed with deionized water several times and then dried by N₂ flow. For tracing the intermediate states, the parallel wafers were extracted out from reacting solution one by one at different time intervals. If there was no specific description, the Cys used in experiments was L-Cys.

Silicon-supported Ag SWs: For silicon-supported Ag SWs, the preparation process was similar to Ag SSs except for a rubbing pretreatment of the silicon surface by tracing papers.

2D patterned silicon-supported Ag NP superstructures: Surface patterning on silicon wafers was fabricated by EBL and RIE. As-prepared patterned silicon wafers were directly put into the Ag⁺/Cys coordination solution and reacted at 37 °C for about 2 days. After reaction, the wafers were rinsed with deionized water several times and then dried by N₂ flow.

Characterization: Attenuated total reflection infrared (ATR-IR) spectra were recorded at 23 °C on Bruker EQUINOX 55. Ag⁺/Cys complexes were extracted from solution, dipped on gold-gilded silicon wafers, and then dried in air. The silicon wafer with Ag SSs was directly used for ATR-IR characterization. The Si content in the reaction solution was measured by

inductively coupled plasma optical emission spectrometer (ICP-OES, THERMO FISHER CO. IRIS Intrepid II XSP). The samples were Ag⁺/Cys coordination solutions containing different silicon wafers (A: pretreated by HF acid; B: with naturally oxidized layer), which were stored in polyethylene (PE) bottles, and then reacted at 37 °C for about 2 days. The purpose for utilizing PE bottle was to avoid the silicon interference from glass. The SEM images of the Ag NP superstructures were obtained by Hitachi S-4800 with an accelerating voltage of 10 kV. Energy-dispersive X-ray (EDX) elemental analysis was accomplished on Horiba EMAX7593-H with an accelerating voltage of 15 kV. Characterizations of TEM and SAED were carried out on Tecnai G² T20 under the accelerating voltage of 200 kV. The sample preparation procedure for the TEM characterization was as follow: the silicon-supported Ag SSs were ultrasonicated and transferred into the deionized water, dipped on copper mesh, and then dried in air. The optical image of the patterns on silicon wafer was obtained by Leica DM4000M. Scattering images and spectra were collected by dark-field microscopy (Olympus BX51) through a × 50 objective (with NA = 0.8, 1 s exposure time). For Raman characterization, PATP powder was dissolved into a mixed solvent of methanol and deionized water with the volume ratio of 1 : 1, and the final concentration was 1.0×10^{-10} M. 100 μL the prepared PATP solution (10^{-10} M) was added into a sample cell and then the silicon wafer with patterned Ag NP superstructures was merged into the PATP solution. SERS signals were collected by laser Raman spectroscopy (Renishaw inVia) through a × 50 objective (with 633 nm laser, ~ 2 mW power, 10 s exposure time).

Additional Experimental Data

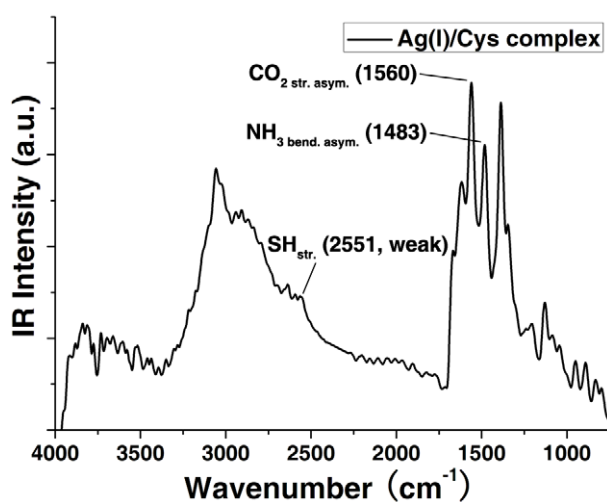


Figure S1. ATR-IR spectrum of the Ag⁺/Cys complex precursors in aqueous solution. The peak of the mercapto group (-SH) is rather weak, which denotes the coordination between Ag and S. Moreover, the carboxyl (-COOH) and amino (-NH₂) groups are obviously red-shift compared with those in free Cys molecules, which denotes that there are associations between the complexes.

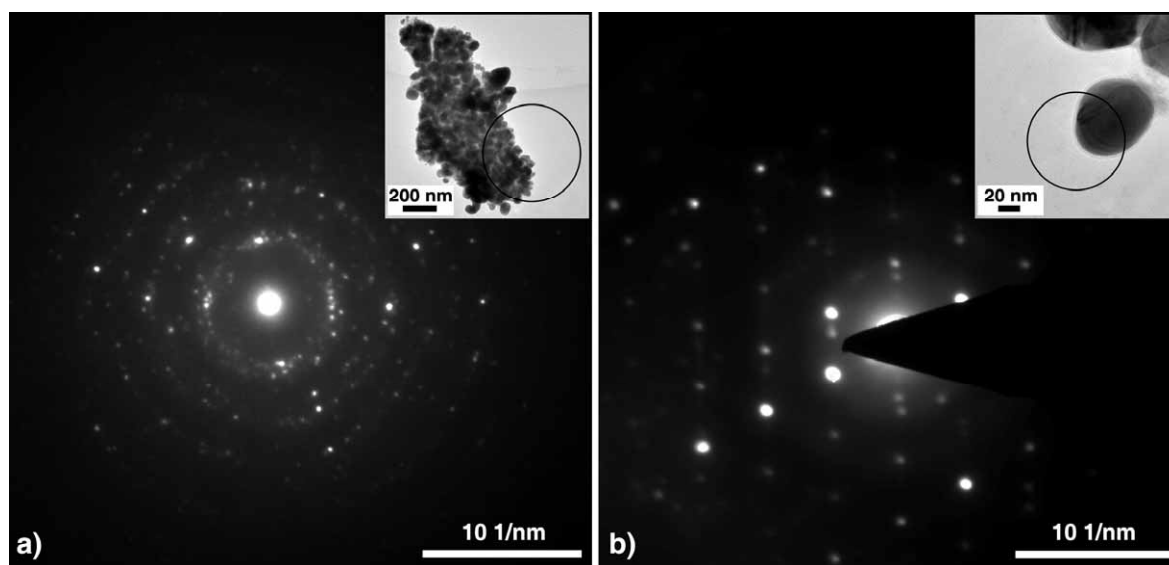


Figure S2. SAED patterns of the Ag SS and the constituent Ag NP. a) Polycrystalline rings observed from Ag SS. b) Typical fcc phase of Ag from a single Ag NP. The calculated lattice constant is 4.06 Å, which is consistent with the JCPDS file ($a = 4.086$ Å, No. 04-0783). Insets are TEM images of the corresponding selected area.

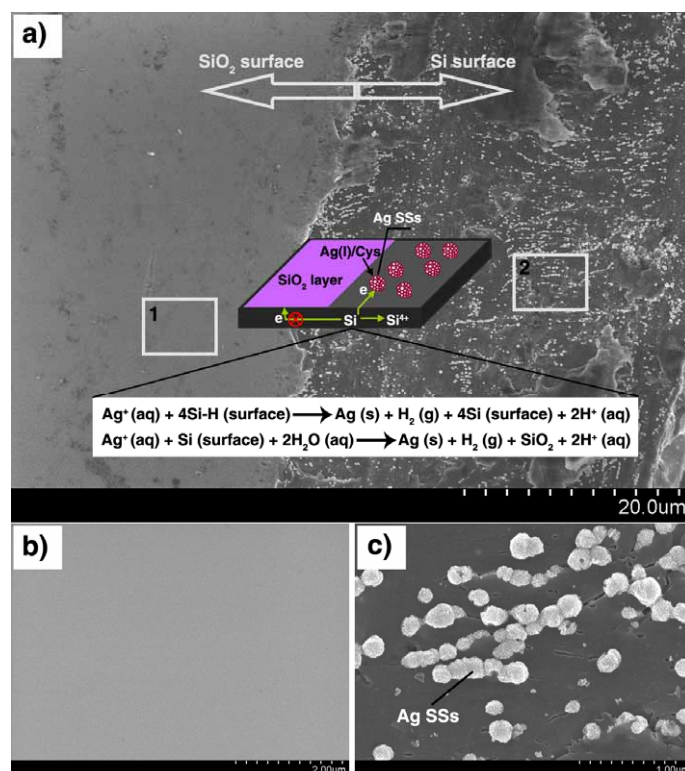


Figure S3. Control experiment on SiO₂/Si heterogeneous wafer. a) Large-area SEM image. The left part is SiO₂ surface, and the right part is Si surface. The inset frames 1, 2 show the corresponding selected areas in b) and c), respectively. The inset figure is a schematic illustration of the selective reduction process of Ag⁺ by the silicon elements on surface. b) Magnifying SEM image of SiO₂ surface. There is no Ag NPs or SSs. c) Magnifying SEM image of Si surface. Comparing b) and c), it is found that the Ag SSs are only generated on silicon surface. The silicon elements on surface act as the reductant for Ag⁺.

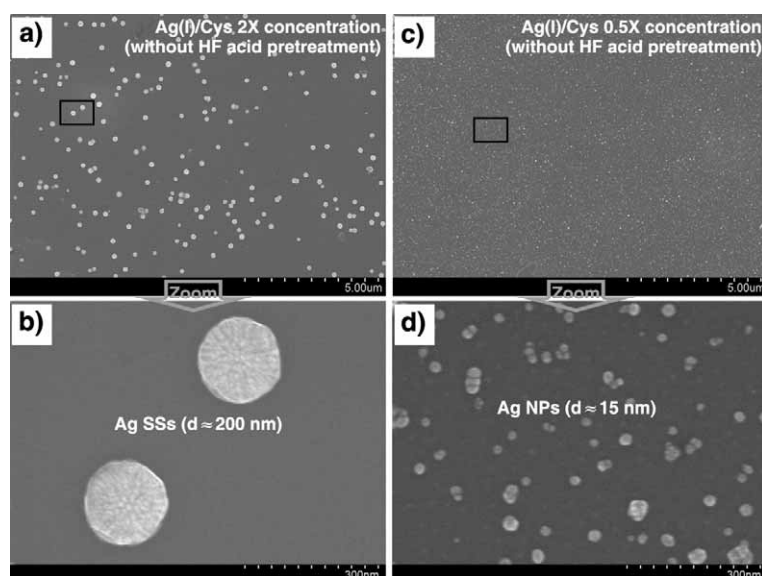


Figure S4. Control experiments with different Ag^+/Cys precursor's concentrations. a) Large-area SEM image of the Ag SSs generated from Ag^+/Cys system with $2 \times$ concentration. b) Magnifying image of the Ag SSs. The typical diameter of the Ag SSs is about 200 nm. c) and d) Large-scale and high resolution SEM images of the Ag NPs generated from Ag^+/Cys system with $0.5 \times$ concentration. The typical diameter of the Ag NPs is about 15 nm.

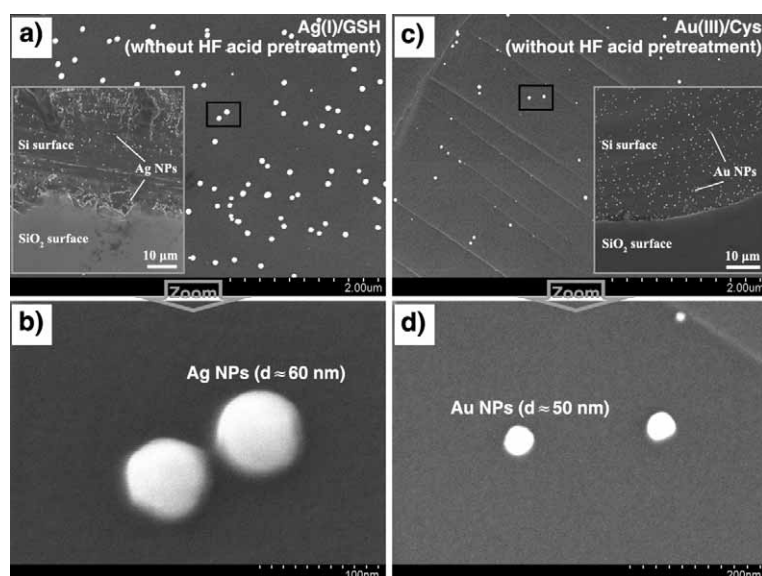


Figure S5. Control experiments with different ligands or metal ions. a) Large-area SEM image of the Ag NPs generated from Ag^+ /GSH system. b) Corresponding magnifying image of the Ag NPs. The typical diameter of the Ag NPs is about 60 nm. c) and d) Large-scale and high resolution SEM images of the Au NPs generated from Au^{3+} /Cys system. The typical diameter of the Au NPs is about 50 nm. Insets in a) and c) show the experimental results on SiO_2/Si heterogeneous wafers. For both Ag^+ /GSH and Au^{3+} /Cys systems, the metal NPs are also only formed on silicon surface.

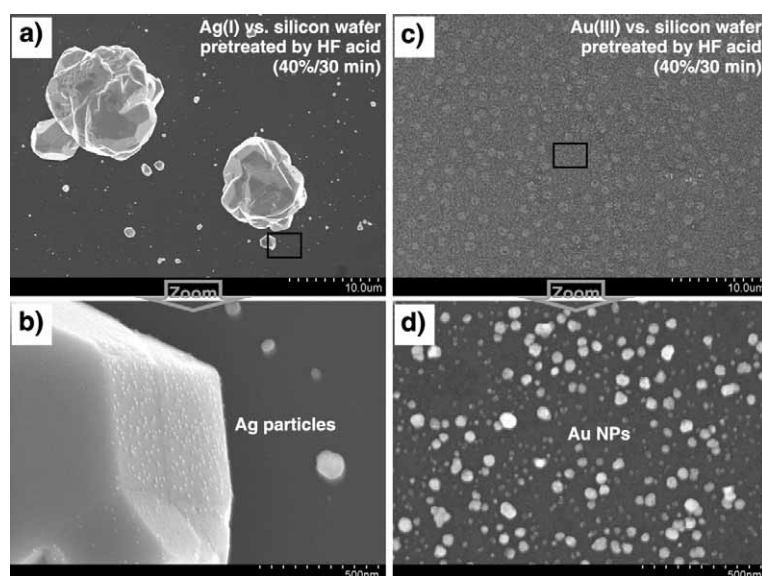


Figure S6. Control experiments with only metal ion precursors. a) Large-area SEM image of the Ag particles generated from blank Ag^+ system. b) Corresponding magnifying image of the Ag particles. The diameter of the Ag particles is not uniform, and there are some big particles. c) and d) Large-scale and high resolution SEM images of the Au NPs generated from blank Au^{3+} system. The diameter of the Au NPs is also not uniform.

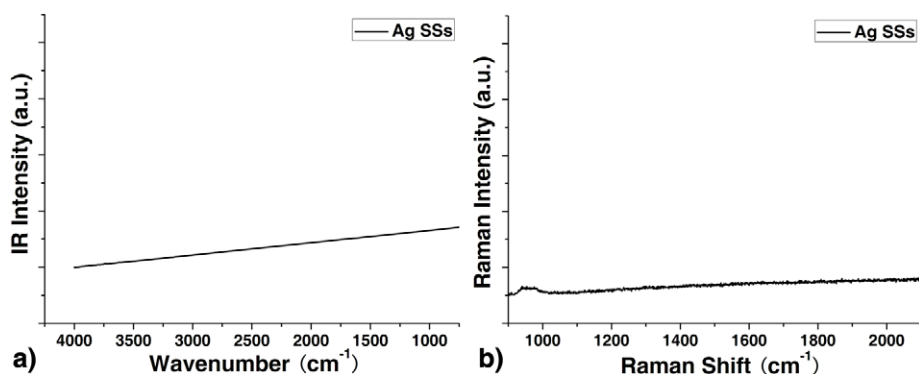


Figure S7. ATR-IR spectrum a) and Raman spectrum b) of the Ag SSs generated from Ag⁺/Cys system. In both spectra, there are no detected signals of Cys molecules or Ag⁺/Cys complexes. This is consistent with the EDX result shown in inset of Fig. 1b, which denotes that there are no organic impurities on the Ag SSs' surface.

Table S1. Dissolved Si from the silicon wafers into the coordination solutions after 2-day reaction detected by ICP-OCS (Rf power: 1150 W; Auxiliary gas flow rate: 0.7 L min⁻¹; Plasma gas flow rate: 0.82 L min⁻¹; Cooling gas flow rate: 14 L min⁻¹).

Sample solutions	Blank (no Si wafer)	A (Si wafer pretreated by HF acid)	B (Si wafer with naturally oxidized layer)
Si concentration (μg mL ⁻¹)	0	1.018	0.541 ^a

^aThe relatively low Si concentration for sample solution B indicates that the freshly generated silicon layer via HF etching is easy to react compared with the naturally oxidized layer. In addition, the mass of Ag SSs per area on bare Si wafer and Si wafer with native oxide shows 16 times difference (Figure 1a). However, the dissolved Si corresponding to the reactions shows only ~2 times difference. The reason for leading to this difference is as follows: As to the bare Si wafer, the reduction of Ag⁺ on silicon surface and the dissolution of Si⁴⁺ into solution take place simultaneously. Whereas, for the Si wafer with native oxide, the

dissolution of Si^{4+} will firstly occurs in the solution to generate the freshly exposed silicon, where the subsequent reduction and formation of Ag Ss will happen.

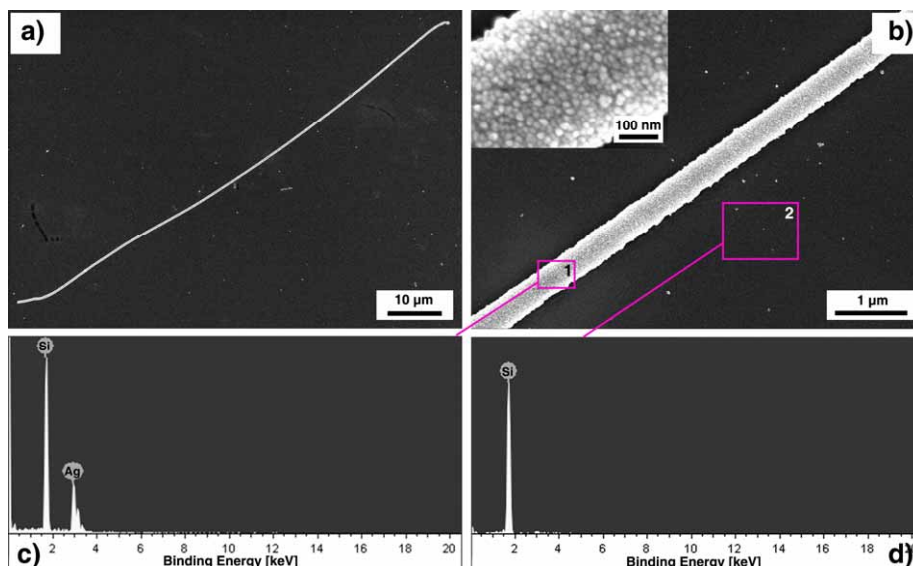


Figure S8. Comparison of the EDX elemental analysis results for different selected areas on the silicon wafer with Ag SW. a) Large-area SEM image of one stick-like Ag SW on silicon surface. b) Selected areas for the following EDX characterizations in c) and d). Inset is the magnifying image of the constituent Ag NPs. c) EDX spectrum corresponding to the selected area 1 shown in b). It denotes that the stick-like SW is Ag without noticeable organic molecules. d) EDX spectrum corresponding to selected area 2 shown in b). There is no Ag signal observed. It reveals that the Ag SWs strictly grow along the rubbing grooves and the intact parts on the silicon surface are strongly screened.

Table S2. Parameters of RIE (SF_6).

Pressure (Pa)	Flow (sccm)	Voltage (V)	Power (W)	Time (s)
3	30	300-400	80	20-30

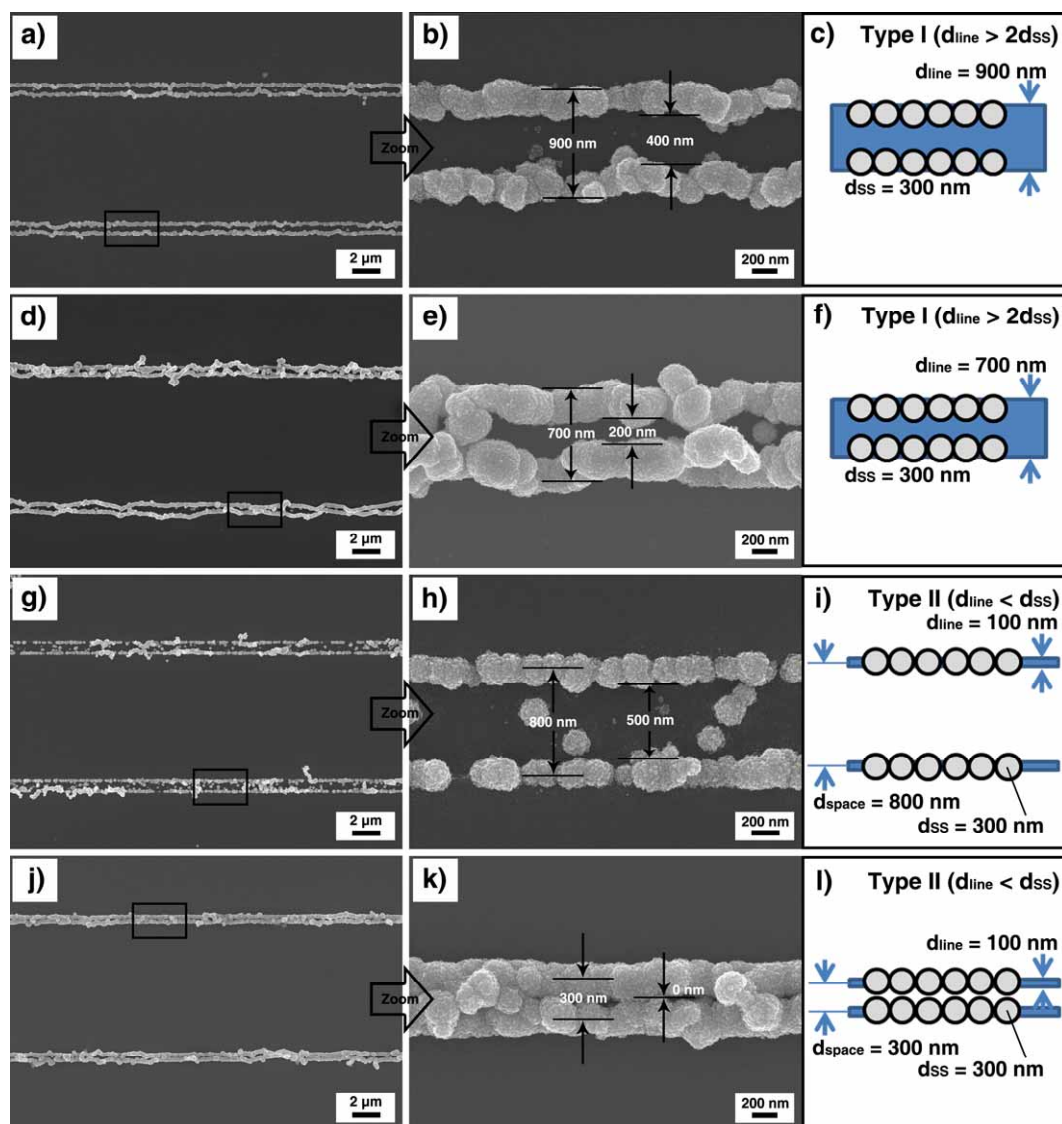


Figure S9. The growth modes of Ag SWs in the etched lines. There are two types of etched line design. In Type I, the line width (d_{line}) is greater than double diameters (d_{ss}) of Ag SSs. In Type II, d_{line} is smaller than d_{ss} . a-c) Type I lines with $d_{\text{line}} = 900$ nm. In this case, Ag SWs preferentially grow along the two edges of the lines. d-f) Type I lines with $d_{\text{line}} = 700$ nm. g-i) Type II lines with d_{line} of 100 nm and inter-line space (d_{space}) of about 800 nm. In this case, Ag SWs preferentially grow along the center axis of the lines. j-l) Type II lines with d_{line} of 100 nm and d_{space} of about 300 nm.

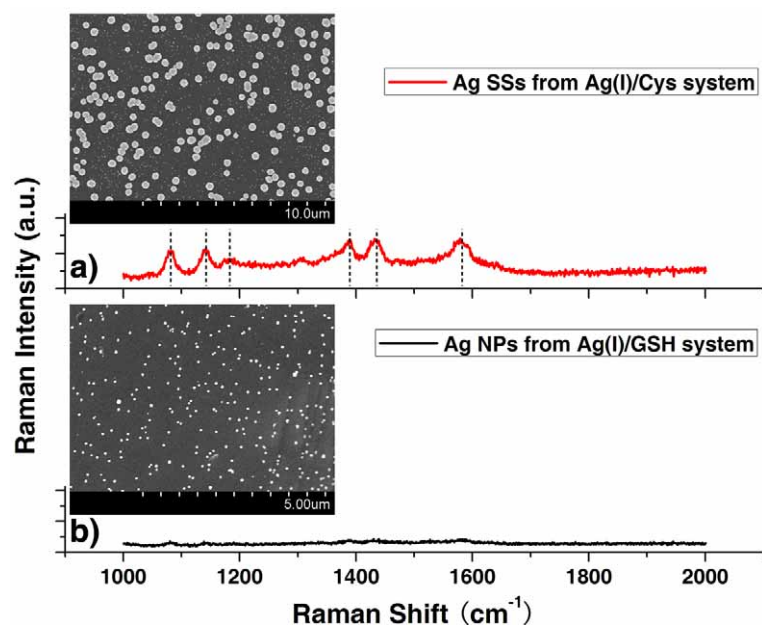


Figure S10. Comparison of the SERS enhancement effects on a) Ag SS substrate obtained by reduction of Ag⁺/Cys complex precursors on silicon wafer (red line) and b) Ag NP substrate obtained by reduction of Ag⁺/GSH complex precursors on silicon wafer (black line). Insets are the corresponding SEM images of Ag SSs and NPs on silicon surface, respectively. The detected molecules are PATP (10⁻¹⁰ M). The dash lines denote the main vibrational peaks of PATP centered at 1080, 1140, 1185, 1387, 1434, and 1581 cm⁻¹.